Analysis for a Dielectrically Filled Parallel-Plate Waveguide with Finite Number of Periodic Slots in its Upper Wall as a Leaky-Wave Antenna

Jong-Ig Lee, *Member, IEEE*, Ung-Hee Cho, *Student Member, IEEE*, and Young-Ki Cho, *Member, IEEE*

***Abstract*—A dielectrically filled parallel-plate waveguide (PPW) with finite number of periodic slots in its upper plate is analyzed as a leaky-wave antenna structure for E-polarization case. The characteristics of the finite periodic structure such as input impedance matching, antenna efficiency, gain, and radiation pattern are investigated. In particular, phenomena such as total reflection and transmission occurring in the practical finite periodic structure, associated with the coupling point and the real solution (propagation constant), respectively, in the fast wave region observed for the infinite open periodic structure case, are described in detail.**

***Index Terms*— Infinite and finite leaky-wave structures, total reflection and transmission.**

I. Introduction

THE leaky-wave radiation problem from a periodically slotted dielectrically filled parallel-plate waveguide (PPW) (or periodic strip grating geometry over a grounded dielectric) has been a subject of several studies [1]–[4]. The problem was analyzed by using the transverse resonance method [1], [2] or by numerically solving the approximated transcendental equation [3] obtained by use of Hertzian potentials under the assumption that the slot or strip width be small compared with a period. Recently a simple method based on the point matching formulation [4] without such constraints was applied to the problem. However most of previous works have been devoted to the analysis of the infinite periodic structure and so the feeding geometry and the finite effect of the structure have not been taken into account. Hence, a solving method for the finite periodic structure is needed.

The main purpose of this work is first to consider an analysis method for this finite case and second to investigate the characteristics of the finite periodic structure, from the viewpoint of a leaky-wave antenna, such as input impedance, antenna efficiency, gain, and radiation pattern.

Manuscript received July 10, 1997; revised April 6, 1998. This work was supported in part by the Institute of Information Technology Assessment and in part by Korea Science and Engineering Foundation under Contract 97K3-0808-03-01-3.

J.-I. Lee is with the Division of Information and Communication Engineering, Dongseo University, Pusan, 617-716, Korea.

U.-H. Cho is with the Department of Electronics and Information, Kyungdong College of Techno Information, Taegu, Korea.

Y.-K. Cho is with the School of Electronic and Electrical Engineering, Kyungpook National University, Taegu, 702-701, Korea.

Publisher Item Identifier S 0018-926X(99)04776-6.

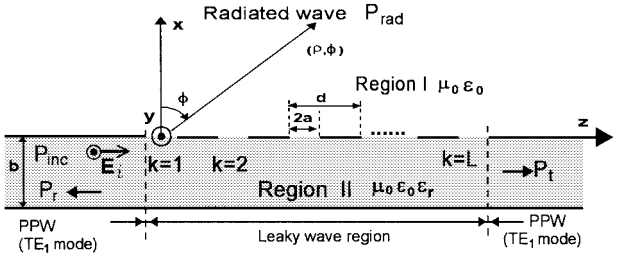

Fig. 1. The leaky-wave structure of finite number (L) of periodic slots in the parallel-plate waveguide filled with a homogeneous dielectric.

II. Formulation

For this purpose, we are to analyze the PPW with finite number of slots in its upper plate as shown in Fig. 1 in connection with a leaky-wave antenna application. In Fig. 1, the excitation and the structure are invariant with respect to the y-direction (i.e., $(\partial/\partial y) = 0$). Regions are divided into free space region (I) over the PPW and the dielectric slab region (II) inside the PPW, each region being characterized by (μ_0, ε_0) and $(\mu_0, \epsilon_0\epsilon_r)$, respectively. The PPW with height b is periodically slotted with period d, slot width $2a$, and finite number L of slots.

The fundamental TE_1 mode, which is only the propagating mode in the unperturbed PPW, is assumed to be incident upon the slotted region as shown in Fig. 1. In this case, the incident electric field $\boldsymbol{E}_i$ is given by $\boldsymbol{E}_i(x,z) = \hat{y}\sin(\pi x/b)\exp[-j\sqrt{k_0^2\epsilon_r - (\pi/b)^2}z]$. Here $\hat{y}$ is a unit vector along the y-axis and $k_0 = \omega\sqrt{\mu_0\epsilon_0}$.

Choosing the appropriate Dirichlet Green functions in each region I, II and applying these to Green's second identity and imposing the continuity of tangential electromagnetic fields through the slots give the following desired integro-differential equation [5], [6]:

$$\sum_{k=1}^{L}\int_{kd-a}^{kd+a}\frac{1}{j2}\left\{\left(k_0^2+\frac{\partial^2}{\partial z^2}\right)H_0^{(2)}(k_0|z-z'|) + \frac{2}{b}\sum_{p=1}^{\infty}\frac{(p\pi/b)^2}{k_0\gamma_p}e^{-jk_0\gamma_p|z-z'|}\right\}M_k(z')\,dz' = \frac{\partial}{\partial x}[E_i(x,z)]\big|_{x=0_-}, \quad \text{over each slot} \tag{1}$$

where $M_k(z')(k = 1, 2, \cdots, L)$ is the z-component magnetic current density over the kth slot $(= E_{ky}; y$-component electric

field), $H_0^{(2)}(\cdot)$ denotes the zeroth order Hankel function of the second kind, and $\gamma_p = \sqrt{\epsilon_r - (p\pi/k_0 b)^2}$.

In order to solve the integro-differential equation numerically, piecewise sinusoidal Galerkin method is employed and the resulting linear matrix equation is found to be

$$[Y_{kn}^{lm}][V_{kn}] = [I^{lm}], 1 \le k, l \le L, 1 \le n, m \le N-1 \quad (2)$$

where the super(sub)script set $\{l,m\}(\{k,n\})$ means the $m(n)$th piecewise sinusoid over the $l(k)$th slot and N is the segment number per each slot. The excitation matrix element is expressed to be

$$I^{lm} = \frac{2k_0\pi}{b} e^{-jk_0\gamma_1 z_{lm}} \frac{\cos(k_0\gamma_1 h) - \cos(k_0 h)}{k_0^2 - (k_0\gamma_1)^2} \quad (3)$$

in which z_{lm} is a location of the center of the mth piecewise sinusoid over the lth slot, h is the segment length ($h = 2a/N = z_{lm} - z_{l,m-1}$). The detailed expressions for the admittance matrix elements are obtained by using the piecewise sinusoidal Galerkin method [6], [7] and so omitted here.

From knowledge of the unknown coefficients V_{kn} of the nth piecewise sinusoid over the kth slot, the complex propagation constant in the present finite structure is defined, in an average sense, by [8], [9]

$$\beta_{\text{av}} - j\alpha_{\text{av}} = \frac{\angle V_{1,N/2} - \angle V_{L,N/2}}{d(L-1)} - j\frac{\ln(|V_{L,N/2}|/|V_{1,N/2}|)}{d(L-1)} \quad (4)$$

where $V_{1,N/2}$ ($V_{L,N/2}$) is the coefficient of the $N/2$th piecewise sinusoid over the first (last) slot and N is chosen to be even for convenience.

By use of the large argument approximation of the Hankel function, the expression for the far-zone electric field $E_I(\rho,\phi)$ due to the equivalent magnetic current source over the finite number of slots is obtained to be

$$E_I(\rho,\phi) = \sqrt{\frac{2}{\pi k_0\rho}} e^{-j(k_0\rho - \pi/4)} \cdot \frac{\cos(k_0 h\sin\phi) - \cos k_0 h}{\sin(k_0 h)\cos\phi} \cdot \sum_{k=1}^{L}\sum_{n=1}^{N-1} V_{kn} e^{jk_0 z_{kn}\sin\phi} \quad (5)$$

from which the radiation pattern $\sigma(\phi)$ and the total radiated power per unit length in the y-direction into free-space region are calculated as

$$\sigma(\phi) = 20\log_{10}\left\{\frac{|E_I(\rho,\phi)|}{|E_I(\rho,\phi)|_{\max}}\right\} \quad [\text{dB}] \quad (6)$$

and

$$P_{\text{rad}} = \frac{1}{2\eta_0}\int_{-\pi/2}^{\pi/2} |E_I(\rho,\phi)|^2 \rho\, d\phi = P_{\text{inc}}\eta_{\text{rad}} \quad (7)$$

where $\eta_0 = \sqrt{\mu_0/\epsilon_0}$ and η_{rad} means the normalized radiated power or the antenna efficiency ($= P_{\text{rad}}/P_{\text{inc}}$) of the present finite leaky-wave antenna. Here P_{inc} denotes the incident power into the slotted region from the left unperturbed PPW region as will be given later in (8).

Employing the Poynting's theorem in the expressions for the fields inside the PPW, the incident power and the reflected (transmitted) power from (past) the slotted region, per unit length in the y-direction, P_{inc} and P_r (P_t), respectively, are expressed as

$$P_{\text{inc}} = \frac{\gamma_1 b}{4\eta_0} \quad (8)$$

$$P_r = P_{\text{inc}}\left(\frac{\pi}{k_0 b^2\gamma_1}\right)^2 \left|\sum_{k=1}^{L}\sum_{n=1}^{N-1} V_{kn} P_{kn}^{-}(k_0\gamma_1)\right|^2 = P_{\text{inc}}\eta_r \quad (9)$$

$$P_t = P_{\text{inc}}\left|1 + \frac{j\pi}{k_0 b^2\gamma_1}\sum_{k=1}^{L}\sum_{n=1}^{N-1} V_{kn} P_{kn}^{+}(k_0\gamma_1)\right|^2 = P_{\text{inc}}\eta_t \quad (10)$$

where

$$P_{kn}^{\pm}(\nu) = \frac{2k_0}{\sin(k_0 h)} \frac{\cos(\nu h) - \cos(k_0 h)}{k_0^2 - \nu^2} e^{\pm j\nu z_{kn}}$$

and $\eta_r(\eta_t)$ denotes the normalized reflected (transmitted) power from (past) the slotted region inside the region II.

By use of (5) and (8), the gain G of the antenna is found to be

$$G = 10\log_{10}[2\pi D/P_{\text{inc}}]\ [\text{dBi}] \quad (11)$$

where

$$D = \frac{\rho}{2\eta_0}|E_I(\rho,\phi)|^2_{\max}.$$

III. Numerical Results and Discussions

For the case that $\epsilon_r = 15, b/d = 0.4, 2a/d = 0.5$, the complex propagation constants in an average sense [by use of (4)] for the finite periodic structure (slot number $L = 60$) have been compared with those, at some sampled points of $k_0 d$, in dispersion diagrams for the infinite periodic case ($L = \infty$) in Fig. 2, where the numbers in the brackets denote the orders of leaky modes and the notation of the complex propagation constant given by $\beta_n = \beta + (2n\pi/d) - j\alpha$ has been used for the infinite periodic case. Here the slot number $L = 60$ for the finite case has been chosen such that the antenna efficiency is made larger than about 90%, when the finite structure behaves as an efficient leaky-wave radiator as in the case of $k_0 d = 2.77$ to be discussed later. Fig. 2 shows that both the results are in good agreement in the fast wave region (between points Ⓓ and Ⓕ) except the narrow region near the coupling point Ⓔ [3], where the radiation angle corresponds to the broadside direction and the attenuation constant α has a sharp minimum as discussed later.

Here, in order to understand more about the discrepancy near the coupling point Ⓔ, let us examine the magnetic current density distribution over the slotted region for the case of $k_0 d = 2.52$ as an example near the coupling point Ⓔ in comparison with that for the case of $k_0 d = 2.77$ as an example of the usual leaky-wave radiation case, shown in Fig. 3(a) and (b), respectively.

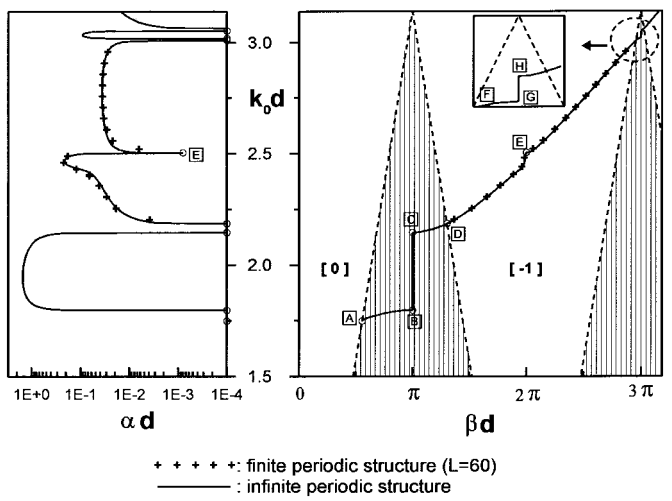

Fig. 2. $k_0 d - \alpha d$ and $k_0 d - \beta d$ diagrams. $\epsilon_r = 15$, $b/d = 0.4$, and $2a/d = 0.5$.

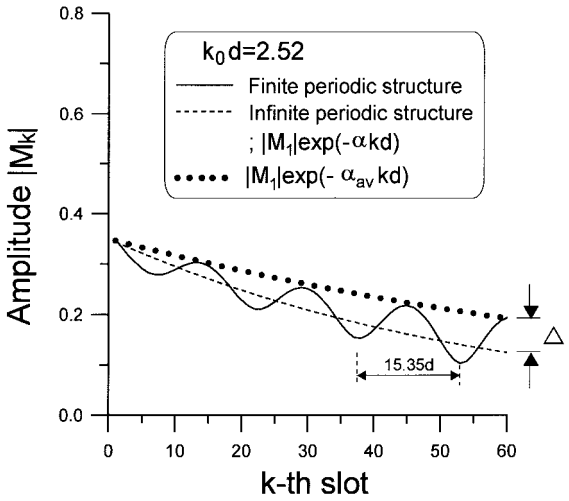

(a)

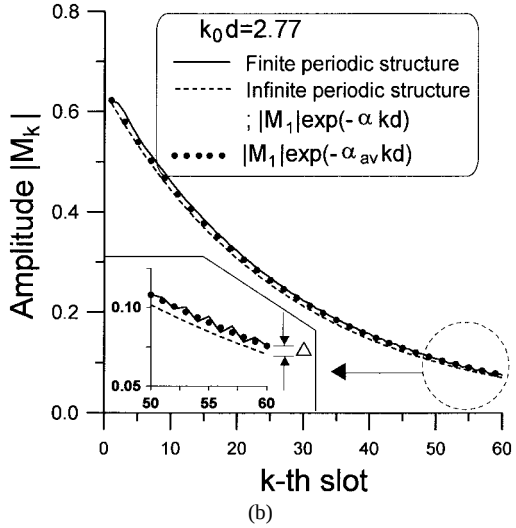

(b)

Fig. 3. Magnetic current density distributions, sampled at the center of each slot. $\epsilon_r = 15$, $b/d = 0.4$, $2a/d = 0.5$, and $L = 60$. (a) $k_0 d = 2.52$ and (b) $k_0 d = 2.77$.

For $k_0 d = 2.52$, $\eta_{\rm rad} = 73.8\%$, $\eta_r = 13.5\%$, and $\eta_t = 12.7\%$, while for $k_0 d = 2.77$ $\eta_{\rm rad} = 98.5\%$, $\eta_r = 0.2\%$, and $\eta_t = 1.36\%$. From this, more reflection due to the impedance mismatching for $k_0 d = 2.52$ is seen to occur at both ends of the slotted region than for $k_0 d = 2.77$. Note also that, for $k_0 d = 2.52$, $\beta_{\rm av} d = 2\pi + \delta_{\rm av} = 6.488$ for the finite periodic structure so that $\delta_{\rm av} = 0.205$, whereas $\beta d = 2\pi + \delta = 6.517$ so that $\delta = 0.234$ for the infinite case, in which case the phase change of all the space harmonics along one period d is given, effectively, by δ (from $\mathrm{Re}[\beta_n d] = 2(n+1)\pi + \delta$). So a pronounced standing wave pattern is formed with period of oscillation very close to a half of $(2\pi/\delta_{\rm av})\ d, 15.35d$ as shown in Fig. 3(a). This pattern is, in shape, very similar to the standing wave pattern observed in the conventional lossy transmission line.

Because the complex propagation constant in an average sense depends on only the initial and final values of M_k by definition, some discrepancy(corresponding to Δ) between $\alpha_{\rm av}$ and α may result as shown in Fig. 3(a). But for the case of $k_0 d = 2.77$ where the finite periodic structure behaves as an efficient leaky-wave antenna, the standing wave pattern becomes relatively undetectable as shown in Fig. 3(b), where slight standing wave pattern is observed to be formed only around the right end of the slotted region from the enlarged view(though the smooth standing wave pattern is not constructed, because the sampling frequency (one per period d) is not enough in comparison with the period of oscillation, a half of $(2\pi/\delta_{\rm av})\ d, 1.85d$). For reference, $k_0 d = 2.77, \beta_{\rm av}\ d = 2\pi + \delta_{\rm av} = 7.979$ so that $\delta_{\rm av} = 1.696$, while $\beta d = 2\pi + \delta = 7.995$ so that $\delta = 1.712$. For the case of $k_0 d = 2.77$, because Δ becomes very small as shown in Fig. 3(b) in contrast to the case of $k_0 d = 2.52$, the complex propagation constants in an average sense become almost the same as those calculated for the infinite periodic case[9] as shown in Fig. 2. For reference, at the coupling point Ⓔ for the infinite periodic case, the attenuation constant α is seen to have a sharp minimum of $\alpha = 0.081\,34$, for which $\alpha d = 8.134 \times 10^{-4}$ in Fig. 2.

Next we are to examine the characteristics such as input impedance matching performance and antenna efficiency over the fast wave region including the coupling point Ⓔ (between points Ⓓ and Ⓕ in Fig. 2) for the finite periodic leaky-wave structure. To this end, the normalized reflected power η_r from the slotted region, the normalized transmitted power η_t to the guide beyond the slotted region, and the normalized radiated power(or antenna efficiency) $\eta_{\rm rad}$ through the slotted region into the upper half free space region with respect to the incident power are illustrated as a function of $k_0\ d$ for the finite periodic leaky-wave structure $(L = 60)$ in Fig. 4. From Fig. 4, most of the incident power is observed to be radiated over the fast wave region between points Ⓓ and Ⓕ except the neighborhood of the coupling point Ⓔ. However at the coupling point Ⓔ, the normalized radiated power $\eta_{\rm rad}$ abruptly goes through a sharp minimum (2.6%) and at the same time, the normalized reflected power η_r also goes through a sharp peak (97%) and so the normalized transmitted power η_t (0.4%) is negligible. From this result, it is seen that almost the total reflection occurs at the junction between the unperturbed PPW region and the slotted (leaky-wave) region when the (leaky-wave) radiation angle corresponds to the broadside direction normal to the finite grating surface.

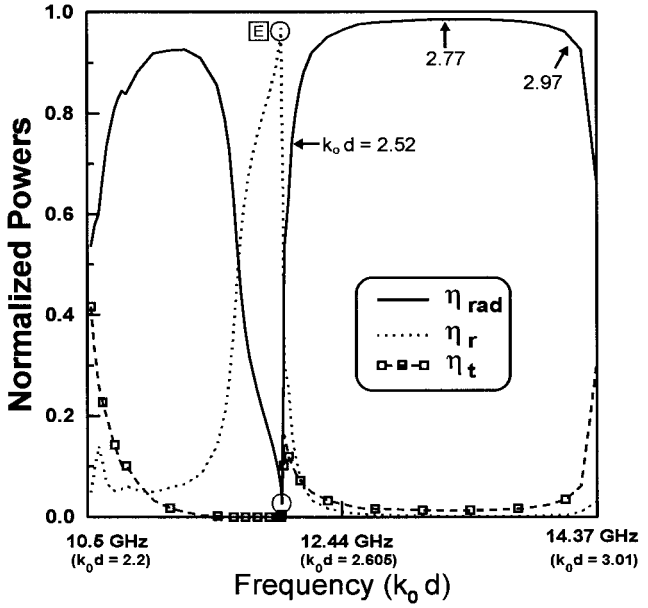

Fig. 4. Normalized reflected (η_r), transmitted (η_t), and radiated $(\eta_{\rm rad})$ powers for the finite periodic structure versus frequency. $\epsilon_r = 15, b/d = 0.4, 2a/d = 0.5$, and $L = 60$.

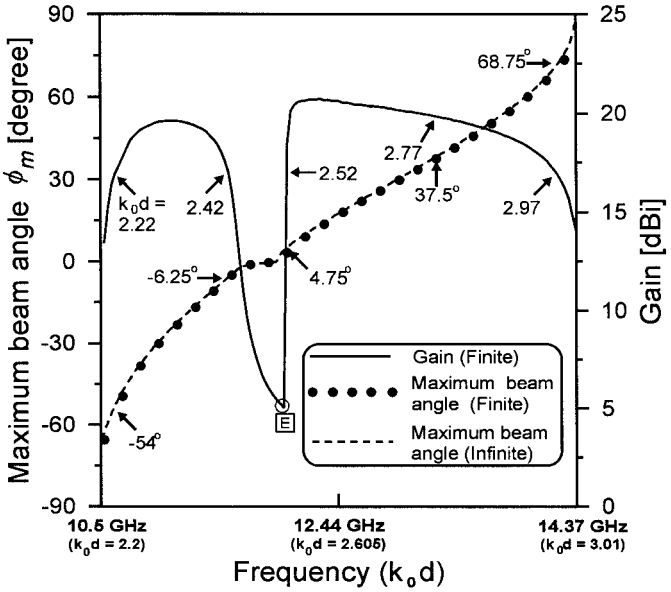

Fig. 5. Antenna gain G, maximum leaky beam angle ϕ_m for the finite periodic structure, and maximum leaky beam angle $\sin^{-1}[\mathrm{Re}(\beta_{-1}/k_0)]$ for the infinite periodic structure versus frequency. $\epsilon_r = 15, b/d = 0.4, 2a/d = 0.5$, and $L = 60$.

In order to further investigate the performance of the present finite leaky-wave structure from the viewpoint of the frequency scanning antenna (FSA), the computed antenna gain and maximum radiation beam angle ϕ_m as a function of frequency are presented (marked with dots) in Fig. 5, where the maximum radiation beam angle given by $\sin^{-1}[\mathrm{Re}(\beta_{-1}/k_0)]$ for the infinite leaky-wave structure case is also presented by the dashed line for comparison. The maximum beam angle ϕ_m in Fig. 5 for the finite leaky-wave structure case has been determined from the radiation pattern obtained by directly integrating the equivalent magnetic current source over the finite number of slots, based upon which the frequency at which the maximum beam angle becomes broadside direction has been determined and the corresponding points have been indicated by Ⓔ in Figs. 4 and 5. The values of β_{-1} $(= \beta - j\alpha - (2\pi/d)$ for the maximum beam angle for the infinite periodic case above are obtained by use of the method in [9].

From the viewpoints of the impedance matching performance and the antenna efficiency as well as the gain performance over the beam scanning range, the present finite structure for the case that the region II inside the guide is filled with the high dielectric material $(\epsilon_r = 15)$ is more suitable for the FSA of forward leaky radiation than the backward leaky radiation (if a broader beam scanning range is desired), as shown in Figs. 4 and 5. From Fig. 5, it is also seen that, if we choose the operating frequency range for the FSA application over which the gain is greater than 17 dBi (for example), the antenna beam scanning ranges from 4.75 to 68.75° as the frequency is varied from 12.03 to 14.18 GHz. For reference, the locations of $k_0 d$ and the maximum beam angle which correspond to 17 dBi gain are indicated in Fig. 5.

In order to examine the radiation characteristics of the present finite leaky-wave structure as the frequency is scanned, radiation patterns at 12.03, 13.23, and 14.18 GHz are illustrated in comparison with those(obtained by use of the method in [9]) for the infinite leaky-wave structure for the case that $L_{\rm slot} = 60\ (= L)$ in Fig. 6. As discussed in [9], $L_{\rm slot}$ means the total slot number counted in the calculation procedure of the radiation pattern for the infinite leaky-wave structure, which is determined so that the radiation pattern does not change appreciably even if larger number of slots than this are taken into account. The maximum radiation beam angles for the finite structure are observed to be very slightly shifted toward broadside direction compared with those for the infinite structure in Fig. 6(a)–(c). Because of the impedance mismatching (though small) at the input feeding end between the left unperturbed PPW and slotted region, the magnetic current density distribution over some slots near the input feeding end become deviated from the typical magnetic current density distribution for the infinite periodic case for which the complex propagation constant is exactly definable unlike the finite periodic structure case where the complex propagation constant is described only in an average sense. This deviation may mainly contribute to differences between maximum radiation beam angles for finite and infinite structure cases. There is another discrepancy observed in the neighborhood of $\phi = -\phi_m$ (marked with circles in Fig. 6) between radiation patterns for the finite and infinite cases. This discrepancy can be explained as: the fundamental leaky-wave traveling in the positive z direction radiates at a maximum beam angle ϕ_m, while the reflected wave due to mismatch in the right end of the finite leaky-wave structure forms a beam in the direction of $\phi = -\phi_m$. This difference can be reduced by increasing the antenna efficiency, that is, by increasing the finite number L of slots.

Let us examine the case where the region II inside the PPW is filled with the low dielectric material. This case is a contrastive example to the high dielectric material case discussed so far. The numerical results(marked with crosses) for the complex propagation constants for the finite periodic case that

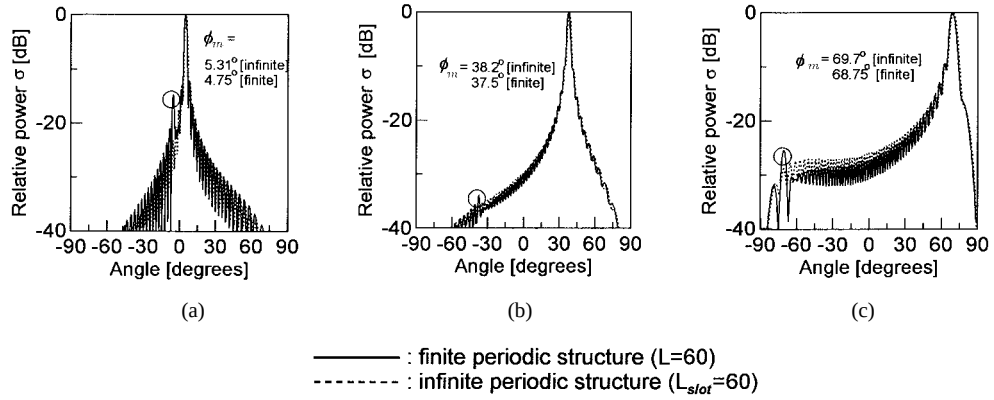

Fig. 6. Radiation patterns. $\epsilon_r = 15$, $b/d = 0.4$, and $2a/d = 0.5$. ———: finite periodic structure with $L = 60$, - - - - - - -: infinite periodic structure with $L_{\rm slot} = 60$. (a) $k_0 d = 2.52$ [12.03 GHz], (b) $k_0 d = 2.77$ [13.23 GHz], and (c) $k_0 d = 2.97$ [14.18 GHz].

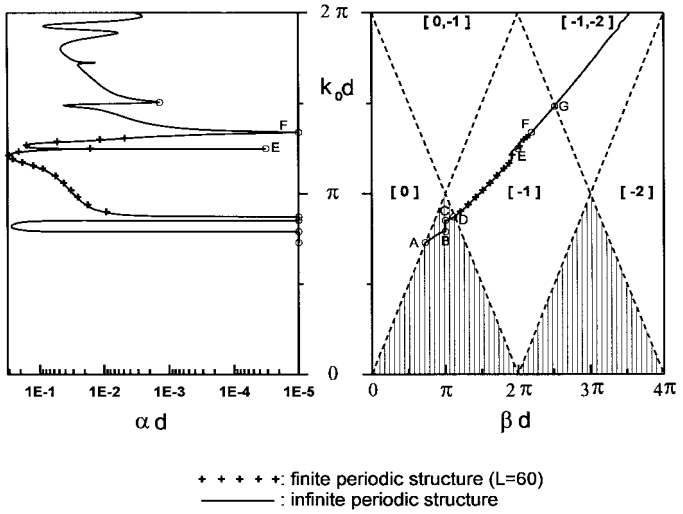

Fig. 7. $k_0 d - \alpha d$ and $k_0 d - \beta d$ diagrams. $\epsilon_r = 3.5$, $b/d = 0.8$, and $2a/d = 0.5$. + + + + +: finite periodic structure with $L = 60$, ———: infinite periodic structure.

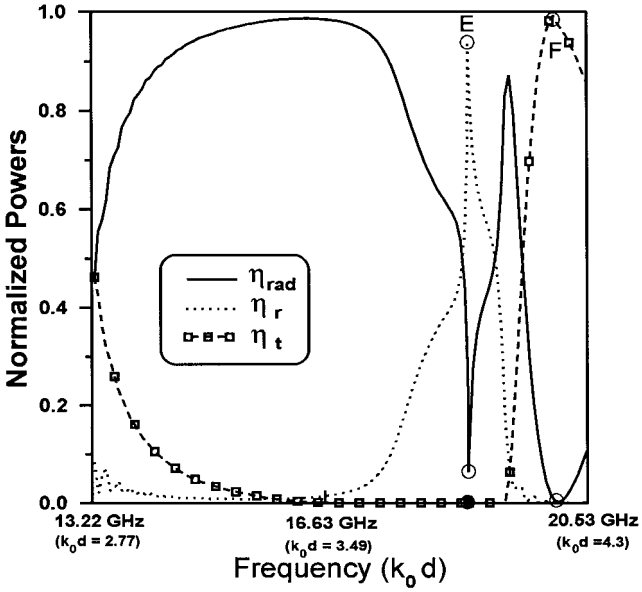

Fig. 8. Normalized reflected (η_r), transmitted (η_t), and radiated ($\eta_{\rm rad}$) powers for the finite periodic structure versus frequency. $\epsilon_r = 3.5$, $b/d = 0.8$, $2a/d = 0.5$, and $L = 60$.

$\epsilon_r = 3.5$, $b/d = 0.8$, $2a/d = 0.5$, and finite number $L = 60$ of slots are compared with those for the infinite periodic case in Fig. 7. In order to further investigate the performance as a leaky-wave antenna as well as a FSA in this case too, the normalized reflected, transmitted, and radiated power versus frequency are illustrated in Fig. 8, in parallel with which the gain performance and the maximum radiation beam angle versus frequency for the finite periodic case are presented in Fig. 9. For the low dielectric substrate case too, almost the total reflection is observed to occur at point E as shown in Fig. 8.

For the case of the real solution [3] (indicated by "F" in Figs. 7–9 in the fast wave region occurring for the infinite periodic structure, the attenuation constant α becomes zero, which means no radiation. So in this case, the incident power in Fig. 1 is expected to be transmitted to the guide beyond the slotted region with negligible radiation. But because the value of $k_0 d = 4.2097$ at "F" in Figs. 7–9 satisfying the condition [3] for the real solution, $b\sqrt{k_0^2 \epsilon_r - \beta_{-1}^2} = 2\pi$, is necessarily larger than the value of $k_0 d = 4.1981$ obtained from the cutoff condition $k_0 d = (1/\sqrt{\epsilon_r})\ (2\pi/b)\ d$ of the first higher order TE_2; mode in the unperturbed PPW, the TE_2 mode is generated at the discontinuities at both ends of the slotted region of the finite leaky-wave structure. Here it is important to note both that the radiated power ($\eta_{\rm rad} = 0.2\%$) for $k_0 d = 4.2097$ is less than that ($\eta_{\rm rad} = 0.5\%$) for $k_0 d = 4.1981$ and becomes minimum, and that the reflected power ($\eta_r = 0.01\%$) calculated from the contribution of only the fundamental TE_1 mode for $k_0 d = 4.2097$ is less than that ($\eta_r = 0.2\%$) for $k_0 d = 4.1981$, which is consistent with "a zero in the attenuation constant α." However as a result of the redistribution of TE_2 mode power to the reflected and transmitted powers, the transmitted power ($\eta_t = 98.8\%$) for the case of $k_0 d = 4.2097$ becomes less than that ($\eta_t = 99.3\%$) for the case of $k_0 d = 4.1981$ but by a very slight amount ($\cong 0.5\%$).

So it seems reasonable to conclude that the real solution (propagation constant) in the fast wave region occurring for the infinite periodic case corresponds to the total transmission phenomenon with inclusion of the TE_2 mode contribution with negligible minimum radiation for the finite periodic case, which contrasts well with the case of coupling point where the

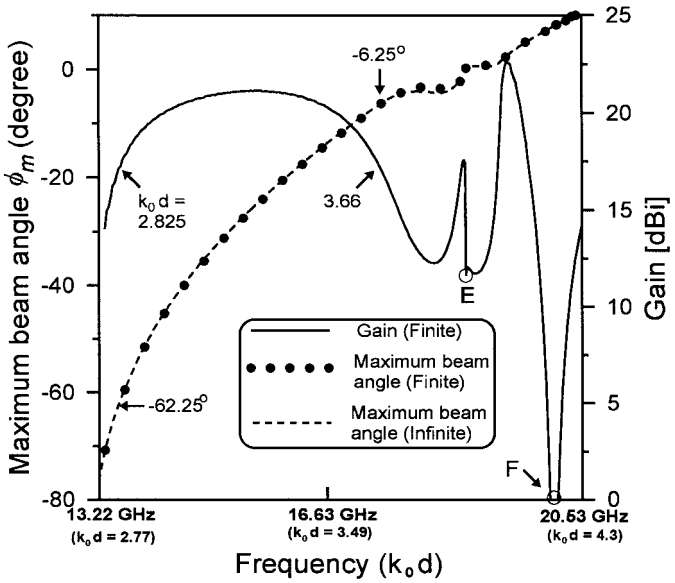

Fig. 9. Antenna gain G, maximum leaky beam angle ϕ_m for the finite periodic structure, and maximum leaky beam angle $\sin^{-1}[\mathrm{Re}(\beta_{-1}/k_0)]$ for the infinite periodic structure versus frequency. $\epsilon_r = 3.5$, $b/d = 0.8$, $2a/d = 0.5$, and $L = 60$.

total reflection phenomenon occurs.

This total transmission phenomenon may result in deterioration of the antenna efficiency (η_{rad}) and gain performance as shown in Figs. 8 and 9, which may constitute a reason why the present finite periodic structure with the low dielectric substrate is unsuitable for the forward radiation as a FSA. It is also seen that, while the range of beam scan angle ($-6.25°$ to $-62.25°$) over which the gain is greater than 17dBi is comparable to that (4.75 to 68.75°) for the high dielectric substrate case discussed above, the corresponding dynamic frequency range should cover almost twice that for the high dielectric substrate case as shown in Figs. 5 and 9.

IV. Conclusion

The problem of leaky-waves emanating from a periodically slotted dielectrically filled PPW for a finite number of slots is analyzed for E-polarization case. The characteristics of the finite periodic (leaky-wave) structure such as impedance matching, antenna efficiency, gain, and radiation pattern are investigated. Some differences between the radiation patterns for the finite and infinite cases are discussed. Also phenomena such as total reflection and transmission occurring in the practical finite periodic structure are described in detail. In addition, an applicability of the finite periodic structure as a frequency scanning antenna is briefly discussed.

References

[1] R. C. Honey, "A flush-mounted leaky-wave antenna with predictable patterns," *IRE Trans. Antennas Propagat.*, vol. AP-7, pp. 320–329, Oct. 1959.

[2] R. E. Collin, "Analytical solution for a leaky-wave antenna," *IRE Trans. Antennas Propagat.*, vol. AP-10, pp. 561–565, Sept. 1962.

[3] J. Jacobsen, "Analytical, numerical, and experimental investigation of guided waves on a periodically strip-loaded dielectric slab," *IEEE Trans. Antennas Propagat.*, vol. AP-18, pp. 379–388, May 1970.

[4] J. A. Encinar, "Mode-matching and point-matching techniques applied to the analysis of metal-strip-loaded dielectric antennas," *IEEE Trans. Antennas Propagat.*, vol. 38, pp. 1405–1412, Sept. 1990.

[5] Y. K. Cho, "Analysis of a narrow-slit in a parallel-plate transmission line: E-polarization case," *Electron. Lett.*, vol. 23, no. 21, pp. 1105–1106, 1987.

[6] C. W. Chuang, "Generalized admittance matrix for a slotted parallel-plate waveguide," *IEEE Trans. Antennas Propagat.*, vol. 36, pp. 1227–1230, Sept. 1988.

[7] J. I. Lee and Y. K. Cho, "Electromagnetic scattering of a Gaussian beam wave from finite periodic slots in a parallel-plate waveguide," in *Proc. Int. Symp. Antennas Propagation*, Chiba, Japan, vol. 1, Sept. 1996, pp. 29–32.

[8] C. W. Lee, J. I. Lee, and Y. K. Cho, "Analysis of leaky-waves from a periodically slotted parallel-plate waveguide for finite number of slots," *Electron. Lett.*, vol. 30, no. 20, pp. 1633–1634, Sept. 1994.

[9] C. W. Lee and Y. K. Cho, "Periodically slotted dielectrically filled parallel-plate waveguide as a leaky-wave antenna for infinite and finite periodic structures," in *Proc. Int. Symp. Electromagnetic Theory*, St. Petersburg, Russia, May 1995, pp. 314–317.

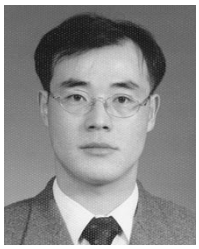

Jong-Ig Lee (S'97–M'99) was born in Andong, Korea in 1967. He received the B.S., M.S., and Ph.D. degrees in electronic engineering from Kyungpook National University in 1992, 1994, and 1998, respectively.

In 1998, he was a Research Professor at the School of Electronics, Kumoh National University of Technology, Kumi, Korea. Currently, he is with Dongseo University, Pusan, Korea, as a full-time Lecturer of the Division of Information and Communication Engineering. His research interests include electromagnetic scattering by periodic structures and planar antenna theory.

Dr. Lee received the 1996 International Symposium on Antennas and Propagation ('96ISAP) "Young Scientist Award." He is a member of the Korea Electromagnetic Engineering Society (KEES) and the Korea Institute of Telematics and Electronics (KITE).

Ung-Hee Cho (S'97) received the B.S. and M.S. degree in electronics engineering from Kyungpook National University, Taegu, Korea, in 1987 and 1989, respectively. He is currently working toward the Ph.D. degree in the School of Electronics and Electrical Engineering, Kyungpook National University.

From 1989 to 1995, he was a Researcher at the Agency for Defense Development, Jinhae, Korea. He is currently a full-time Lecturer in the Department of Electronics and Information, Kyungdong College of Techno Information, Taegu, Korea. His research interests include computational electromagnetics, antenna theory, and EMI/EMC.

Young-Ki Cho (M'87) was born in Seoul, Korea, on September 12, 1954. He received the B.S. degree in electronics engineering from Seoul National University, Seoul, Korea, in 1978, and the M.S. and Ph.D. degrees in electrical engineering from the Korea Advanced Institute of Science and Technology, Taejon, Korea, in 1981 and 1997, respectively.

Since 1981, he has been with Kyungpook National University, Taegu, Korea. Currently he is a Professor in the School of Electronics and Electrical Engineering, Kyungpook National University. His research interests include electromagnetic scattering and radiation problems in the general periodic structure and antenna array theory.

Dr. Cho is a member of the Korea Electromagnetic Engineering Society (KEES), Korea Institute of Communication Science (KICS), and Korea Institute of Telematics and Electronics (KITE). He is also a member of Commission B (Fields and Waves) of the International Union of Radio Science (URSI).